Performance investigation of the bed adsorption of an adsorption desalination using CFD simulation

Mohamad Hossein Bakhshandeh · Taleb Zarei · Jamshid Khorshidi · M H Bakhshandeh · T Zarei · J Khorshidi

Received: date / Accepted: date

Abstract One of the critical elements of an adsorption desalination system is the adsorption bed. System dynamics of a 2-bed single-stage silica gel plus water-based AD system was analyzed. A great pattern is expanded using energy conservation and mass connected with the kinetics of the adsorption/desorption process. Computational fluid dynamics (CFD) modeling was handled for simulation of the adsorption process for a rectangular finned tube-based adsorption bed featured with silica gel adsorbent substance. For the simulation, the adsorbents were considered as a solid volume with defined porosity based on Darcy equation. The adsorption and desorption mode of the adsorption bed was simulated. The CFD techniques were then applied to study fin thickness and fin height. The results showed that decreasing the fin thickness increased the water uptake by up to 8% and decreased the fin height from 30mm to 20mm, which resulted in an increase of the water uptake up to 17%. The CFD technique was also used to investigate the effect of plate type on the adsorption bed performance. The results showed that the copper plate improved the water uptake up to 9%. The copper plate decreased the temperature of the adsorption bed up to 11% more than the aluminum plate.

Keywords "Adsorption bed CFD Rectangular finned tube Fin thickness Plates type"

1 Introduction

Nearly, 97% of surface water on the earth is comprised of saltwater, which cannot be applied for drinking or other usage. It is possible to segregate soluble salts and other minerals from water using water desalination processes. Feedwater sources may have seawater, brackish, groundwater, wastewater,

---

Mohamad Hossein Bakhshandeh
Department of Mechanical Engineering, University of Hormozgan, Bandar Abbas, Iran

Taleb Zarei
Department of Mechanical Engineering, University of Hormozgan, Bandar Abbas, Iran E-mail: talebzarei@hormozgan.ac.ir

Jamshid Khorshidi
Department of Mechanical Engineering, University of Hormozgan, Bandar Abbas, Iran E-mail: jkhorshidi@yahoo.com

and process water. Lately, adsorption technology has been used for the desalination of water using minimal energy consumption. The salinity level of 10 ppm requires a running cost of 0.2 $/m and CO2 dissemination of 0.6 kg/m. In addition to water production, the cooling effect can be used for air ventilation systems. The main supremacy of adsorption technology is the possibility of using low-grade waste heat sources (50 – 85C) or solar energy and environment-friendly refrigerants to lower the cost to one-fifth. The adsorption desalination system is featured with four consecutive processes named adsorption, desorption, evaporation, and condensation. Seawater is evaporated in the evaporator through adsorption by the dry adsorbent material along with heat extraction from the chilled water that passes the evaporator coil and cools down the coil. Water vapor is adsorbed in the adsorption process using adsorbent materials and the desorption. The process is featured with regenerating water vapor using the waste heat. Afterwards, the desorbed water vapor is condensed using a condenser to obtain fresh water. Several adsorption pairs have been investigated by various researchers. Silica gel- water double has demonstrated a few advantages, mostly in terms of thermal efficiency and environmental trace. Water is an ideal refrigerant due to its high bosomed heat of evaporation, thermal consistency at high temperature, and good compatibility with a wide range of materials. Silica gel as an adsorbent for water vapor has superior thermal properties of low generation temperature and high adsorption kinetics.

Researches on applying numerical simulations have found helpful and efficient techniques for adsorption systems design and adsorption cycles. Adsorption cooling systems used for automotive applications have already been investigated. Zhang (2000) carried out experiments on an adsorption cooling system using exhaust gas from a diesel engine. Lambert and Jones (2006) designed an automotive adsorption air conditioner using exhaust waste heat and found that an adsorption cooling system can lower fuel consumption; however, the whole mass volume was increased. Tamainot-Telto et al. (2006) described a compact sorption generator based on activated carbon-ammonia pair driven by waste heat obtained from the engine coolant water, giving a cooling power equal to 1.6kW and COP equal to 0.22. Boer et al. (2009) designed an adsorption chiller and conducted on-board testing, with cooling power enough to maintain convenient temperature levels. Zhong et al. (2011) introduced a model to simulate an adsorption air conditioning system based on zeolite-water pair for heavy-duty transport. Vasta et al. (2012) also proposed an automotive adsorption cooling system which gave a COP of 0.25-0.45. Freni et al. (2012) studied the dynamics of the adsorption process of water by loose silica grains utilizing the CFD method.

Thu et al. (2013) examined the efficiency of the ADS using diverse heat recovery designs with two or four-bed modes. The ADS performance was also measured with heat recovery from the condenser to the evaporator or integrated evaporator condenser unit. There was an increase in the evaporator temperature and the adsorption bed pressure because of heat recovery from the condenser, which created an increase in water production. The increase can be three times higher than the standard ADS.

Authors have tried to use adsorption technology for water desalination and cooling based on silica gel and several cycle configurations. The performance of a four-bed silica gel adsorption desalination system was examined in an empirical study by Wang et al. (2019) to study the effects of hot, cold, and chilled water temperatures and cycle duration on the production rate of water cycle coefficient of proficiency.

The adsorption bed is one of the most significant parts of desalination and the most effective element in the performance of the system. An important part that has not received adequate attention in previous researches is the effect of the type of absorbent plates on the adsorption process. Choosing the best material plays an important role in improving system performance.

The use of materials with better conductivity is effective in the improvement of the heat transfer process and increment of the adsorption coefficient.

Absorption Process simulation is very significant to obtain the best answer compared to the real model. The effect of different operation variables (e.g. cooling water flow rate, dry adsorbent desorption time, desorption time, adsorption time, and temperatures of evaporation and condensation) on the performance was an important part of the desalination system. However, previous works have not paid enough attention to this issue. The adsorption system performance was examined with different cycle times, heating fluid temperatures, and flow rates. In addition, the effect of different adsorber bed fin numbers and fin height were examined using the model.

A numerical investigation was conducted on the performance of a prototype adsorption desalination (AD) plant. The key objective is to propose a design and CFD simulation of a novel compacted copper fin heat exchanger with a silica gel adsorbent bed that constitutes a part of the adsorption system. The proposed heat exchanger design is featured with a wide surface area. By estimate, this surface helps to improve the coefficient of performance (COP) of the adsorption phase. It also improves heat transfer in this system arrangement Thu et al. (2020).

The simulation was to examine the fin thickness and fin height effect on the performance of the adsorption bed. The plate type and different materials affected the performance of the system.

2 Mechanism of the present bed adsorption system

Almost every adsorption system relies on a two-bed cycle (Fig. 1). The thermodynamic cycle is demonstrated in Figure 1. There are two adsorber beds in a two-bed cycle system and these beds function in opposite modes. Mainly, during the switching, while an adsorber is in a preheating process, the other one is in a precooling process.

The system includes an evaporator, two adsorption beds, and one condenser. The system work is featured with two processes: adsorption and desorption. When repeated one after another, the system produces desalinated water. Based on this design, the condenser and evaporator are connected to the adsorption beds. During desorption occurs, control valve connects the beds to the condenser. In addition, desalinated water is collected in a tank. The process cycle is completed by connecting the evaporator to the absorption bed. Following adsorption bed saturation, the control valves connecting the adsorption bed and the evaporator are closed. Then, the adsorption bed is heated by the heat exchangers. The temperature and pressure of the adsorption bed increase in the heating process. There is a connection between the adsorption bed and the condenser, where the vapor is condensed by its heat exchangers. After increasing the doping of seawater in the evaporator, a portion of it can be separated.

Fig. 1

3 Adsorption isotherm models

The adsorption isotherm clarifies the amount of adsorbate adsorbed using the adsorbent at a given temperature. The adsorbate mass normalization with the absorbent mass for different materials allows the collation of absorption capability. In this way, we make sure that by implementing the saturation pressure, adsorption stops because of the limited capacity of the empty holes on the surface of the adsorbent. The linear driving force equation (LDF) is the first choice to describe the adsorption kinetics of adsorption working couples. However, there are different adsorption isotherm equations available by Liu (2008).

Adsorption processes can be applied in applications like separation and air-conditioning. It relies on water vapor physical uptake of the surface of the

adsorbent based on Van der Waal's or polar bonding forces (e.g. silica gel, and zeolite). Evaporation of pre-treated seawater happens via the suction trace from the adsorbent which does not need high pressure or temperature in the evaporating unit. After the adsorption of the vapors by the adsorbent, the adsorption heat is returned to the cooling water circuit goes back to the adsorber bed. This adsorption process goes on while the cycle time is not over. For adsorbent regeneration, the bed is supplied with low-temperature waste at the on-set of the desorption mode. Then the desorber is connected to the condenser and the water vapor condensation on the cooler tube surfaces takes place and water is collected on the muster reservoir.

3.1 Computational domain of the simulated adsorption bed

Rectangular finned tube adsorption beds are available in the market with tubes and rectangular fins (Figure 2). The bed design utilized in the silica gel/water adsorption system was manufacture by Weatherite ltd (2020).
The fins dimensions are 115×30×0.105mm and an extra four tubes were uniformly distributed in the width of the adsorption bed. The external diameter of the bed is 15.8mm and thickness of wall is 0.8mm. To have higher thermal conductivity, copper tubes were used. In addition, adsorbent granules were packed between the fins. The cooling water in the adsorption process grows through tubes and decreases the temperature of the adsorption bed and compensates the heat of the of desorption process (Table1.) The cooling water in the adsorption process goes through tubes to decrease the temperature of the adsorption after the desorption process. Silica gel granules are added between fins.

Table 1

Fig. 2

4 CFD model

Equation (1) presents the Darcy equation. Darcy equation that justifies the continuity of the adsorption process and eq. (2) represents the energy equation.

$$\frac{\partial(\varepsilon_s \rho_w)}{\partial t} + \nabla.(\rho_w u_w) = -\frac{\partial(\rho_s w)}{\partial t} \tag{1}$$

$$\rho C_P \frac{\partial T_{bed}}{\partial t} + C_{P_w} \nabla.(T_{bed} \rho_w u_w) = \nabla.(k_s \nabla T_{bed}) + \rho_S \Delta H_s \frac{\partial w}{\partial t} \tag{2}$$

$$u_w = -\frac{\kappa}{\mu} \nabla P_w \tag{3}$$

$$\rho C_P = (\varepsilon_s \rho_w + \rho_s w) C_{P_w} + \rho_s C_{P_s} \tag{4}$$

Where ε_s is porosity of adsorbent bed packed with silica gel granules equal to 0.5 for [23,24], u_w represents water vapour velocity (eq. (3)), ∇P_w represents water vapour pressure gradient, ρc_p is obtained by eq. (4), and k_s is the thermal conductivity of the bed, equal to 0.198 W/(m·K).κ is the

permeability of silica gel and it was determined by eq. (5).

$$\kappa = -\frac{4\varepsilon_s^3 R_p^2}{150(1-\varepsilon_s)^2} \tag{5}$$

Where w is the uptake value of the water vapour that is done by silica gel, which is obtained by the linear driving force (LDF) kinetic model (eqs. (6-7)).

$$\frac{dw}{dt} = K(w_{max} - w) \tag{6}$$

$$K = 15D_{so}\exp\left(\frac{-E_a}{RT_{bed}}\right) / R_P^2 \tag{7}$$

Where w_{max} is the maximum water vapor uptake of silica gel granules at the equilibrium condition. For equation 6, K is the overall mass transfer rate of the silica gel-water pair which can be calculated using equation 7, where D_{SO} represents the pre-exponential constant, E_a stands for the activation energy, R_p stands for the silica gel granule radius and R is the ideal gas constant with their values shown in Table 2.

Table 2

The modified Freundilich model yields this value (eqs. (8-10)) and Table 3 lists the values of constants [23, 24]. (8)(9)(10)

$$W_{max} = A\left[\frac{PT_e}{PT_{bed}}\right]^B \tag{8}$$

$$A = A_0 T_{bed} + A_1 T_{bed} + A_2 T_{bed}^2 + A_3 T_{bed}^3 \tag{9}$$

$$B = B_0 T_{bed} + B_1 T_{bed} + B_2 T_{bed}^2 + B_3 T_{bed}^3 \tag{10}$$

Table 3

4.1 Boundary conditions

The thermal and flow variables on the boundaries of the physical model are determined by the boundary conditions. There are some boundary conditions:

. Flow outlet and inlet boundaries: velocity inlet, pressure inlet, and pressure outlet.

· Recuring, wall, and limit boundaries: wall, symmetry Internal fluid, solid

· Internal face boundaries: wall, porous, and internal

· Internal fluid, solid

The comparison of different mesh grid size is shown in Fig. 3. The average bed temperature and average deviations of the water vapor uptake of three replications are shown. The figure shows that the varying meshing densities have no influence on the prediction of finite element modelling prediction.

In the case of geometry under study, a set of grids is used with CFD computations and the effect of each grid level is analyzed afterwards. To solve the problem, we need a systematic gridding known as the grid convergence or mesh refinement study.

Three mesh types(large- medium-fine) including coarse to dense meshes were generated to make sure that the simulation results were grid-independent adequately. The bed temperature results are shown in Fig. 3. The results shows that the two types of mesh grid (medium and fine grid) was very similar and the error level was less than 3%. Medium mesh is used for simulation to save time and energy.

Fig. 3

5 Results and discussion

5 1Model Validation

The simulation model is validated by applying the experimental outcomes [23,24]. The difference between the experimental data and simulation result is shown in Figure 4. The results show a difference of less than 5%. Figure 4 illustrates the portended and experimental results about average bed temperature, water uptake, and cooling water outlet temperature in an adsorption cooling system based on a SAPO-34/water working pair. The results indicate a good consistency between the finite element model and the experiments.

Fig. 4

5 2Adsorbtion mode

To examine the adsorption process of adsorption bed featured with a rectangular finned tube based on CFD modeling technique, a simulation was performed (inlet water temperature of 30C, evaporator temperature of 15C, and initial bed temperature of 60C). The complete adsorption process took 500s which allowed us to predict the adsorption performance of adsorption bed of silica gel-water working pair.

Figure 5(a) shows the distribution of predicted temperature on the last fin of the rectangular finned tube adsorption bed after 100s, 300s, and 500s. The bed temperature is the average temperature of the adsorption bed which includes the metal and silica gel granules. As illustrated in the figure, the longer the time of simulation the closer the temperature of the last fin to the coolant temperature.

Specifically, when the adsorption process occurs, the average bed temperature decreases with the increase of time. This increase is with a sharp slope between the time of 0 to 200 seconds.

Fig. 5 (a), (b)

The predicted water uptake rate of the plane was investigated at time intervals of 0 to 500 seconds. Obviously, when the desorption process occurs, the water uptake rate becomes a larger with longer simulation time. This is because that the desorption (from time of 50 to 300 seconds) process is fast at the beginning and deaccelerates between 200 to 500 seconds.

Fig. 6 (a), (b)

The horizontal cut plane of a temperature distribution of the last fin in desorption is shown in Figure 7(A). The predicted temperature distribution of the plane was investigated at time intervals of 1, 50, 100, 200 seconds. Clearly, the temperature becomes larger with the increase of time.

Fig. 7 (A), (B)

Figure 7(B) shows the horizontal cut plane of a temperature distribution of the last fin in adsorption. The predicted temperature distribution of the plane was examined at time intervals of 1, 50, 100, 200 seconds. Obviously, from the figure that the temperature decrease with the increase of time.

Fig. 8

Figure 8 shows the desorption process that starts with a bed temperature equal to 30°C and hot water temperature of 60°C.

Fig. 9

It can be noted that water uptake rate increases with decreasing the fin thickness. Clearly, water uptake rate for fin thickness of 1 mm is higher than the others. This can be attributed to that through decreasing the fin thickness, the amount of the adsorbent would increase and hence the ratio between the adsorbent and the metal mass would also increase causing a poorer heat transfer rate.

The results showed that decreasing the fin thickness increases the water uptake by up to 8%. This can be effective in improving system performance.

Fig. 10

Figure 10 shows the water uptake rate increases with decreasing the fin heights. It is clear that the water uptake rate for fin heights of 10 mm is higher than the others. Decreasing the fin height from 30mm to 10mm results in increasing the water uptake by up to 17%. This could be due to the increase in the number of fins and the heat transfer area thus cooling the bed more effectively and increasing the water adsorption by the silica gel.

Fig. 11 (a), (b)

One of the new features of the present study is to compare the result of simulation with different plate types (aluminum plate and copper plate). Figure 11(a) shows the adsorption process with an initial bed temperature of 303k and hot water temperature of 331.4k. The time duration of the process was about 350s. Results showed that copper plate had better adsorption. The copper plate decreases the temperature of the bed by about 11%.

The CFD technique was used to examine the effects of plate types on the performance of the adsorption bed. The results showed that copper plate increased the water uptake up to 9%. Figure 11(b) shows that the copper plate has better performance in increasing the water uptake rate.

6 Conclusion

CFD simulations technique proved to be a powerful tool to examine the

adsorption process and improve the designs of adsorption beds. In this study, the simulation of the adsorption process for a silica gel-water pair in a rectangular finned tube bed structure that can be used for the adsorption desalination system was carried out. The bed geometry and the adsorption process of the working pair were modeled using CFD techniques in COMSOL Multiphysics software.

Simulations were used to investigate the bed performance of adsorption process. The CFD technique was used to examine the effect of fin thickness and fin height on the performance of the adsorption bed. The results showed that decreasing the fin thickness increased the water uptake up to 8%. In addition, decreasing the fin height from 30mm to 20mm resulted in an increase in the water uptake up to 17%. The CFD technique was used to examine the effect of plate types on the performance of the adsorption bed. The results showed that copper plate improved the water uptake up to 9%. Moreover, the copper plate decreased the temperature of the adsorption bed up to 11% more than the aluminum plate.

In conclusion, CFD is a valuable tool to examine the heat transfer behavior of an adsorption bed. Future studies on CFD can use bigger silica gel and porous media and examine if they yield the same outcomes.

Nomenclature

CFD Computational fluid dynamics
COP Coefficient of performance

Symbols

A_0 Constant coefficients for equation 9
B_0 Constant coefficient for equation 10
C_P Specific heat
C_{SO} Pre-exponential constant
d Diameter
E_a Activation energy
f Friction factor
h Specific enthalpy
∇H Heat of adsorption

k Thermal conductivity
K Overall mass transfer rate
M Mass
N Number

References

Freni, A. et al. (2012). “Simulation of water sorption dynamics in adsorption chillers: One, two and four layers of loose silica grains”. *Applied Thermal Engineering* 44, pp. 69–77. DOI: 10.1016/j.applthermaleng.2012.03.038. URL: https://dx.doi.org/10.1016/j.applthermaleng.2012.03.038.

Lambert, M A and B J Jones (2006a). “Automotive Adsorption Air Conditioner Powered by Exhaust Heat. Part 1: Conceptual and Embodiment Design”. *Proceedings of the Institution of Mechanical Engineers, Part D: Journal of Automobile Engineering* 220(7), pp. 959–972. DOI: 10.1243/09544070jauto221. URL: https://dx.doi.org/10.1243/09544070jauto221.

Thu, K et al. (2013).

Vasta, Salvatore et al. (2012). “Development and lab-test of a mobile adsorption air-conditioner”. *International Journal of Refrigeration* 35(3), pp. 701–708. DOI: 10.1016/j.ijrefrig.2011.03.013. URL: https://dx.doi.org/10.1016/j.ijrefrig.2011.03.013.

Z Zhang, L (2000). “Design and testing of an automobile waste heat adsorption cooling system”. *Applied thermal engineering* 20(1), pp. 103–114.

Zhong, Yongfang, Tiegang Fang, and Kevin L. Wert (2011). “An adsorption air conditioning system to integrate with the recent development of emission control for heavy-duty vehicles”. *Energy* 36(7), pp. 4125–4135. DOI: 10.1016/j.energy.2011.04.032. URL: https://dx.doi.org/10.1016/j.energy.2011.04.032.

Ali, S M and A Chakraborty (2016). “Adsorption assisted double stage cooling and desalination employing silica gel+ water and AQSOA-Z02+ water systems”. *Energy conversion and management* 117, pp. 193–205.

Alsaman, Ahmed S. et al. (2017). “Performance evaluation of a solar-driven adsorption desalination-cooling system”. *Energy* 128, pp. 196–207. DOI: 10.1016/j.energy.2017.04.010. URL: https://dx.doi.org/10.1016/j.energy.2017.04.010.

Amirfakhraei, Amirhossein, Taleb Zarei, and Jamshid Khorshidi (2020). “Performance improvement of adsorption desalination system by applying mass and heat recovery processes”. *Thermal Science and Engineering Progress* 18, pp. 100516–100516. DOI: 10.1016/j.tsep.2020.100516. URL: https://dx.doi.org/10.1016/j.tsep.2020.100516.

Boer, R De, S F Smeding, and S Mola (2009). *Silicagel-water adsorption cooling prototype system for mobile air conditioning*. Petten: ECN. ---2

Singh H, Cai J (2018) A mechanistic model for multi-scale sorption dynamics in shale. DOI 10.1016/j.fuel.2018.07.104, URL https://dx.doi.org/10.1016/

j.fuel.2018.07.104

Lambert, M A and B J Jones (2006b). “Automotive Adsorption Air Conditioner Powered by Exhaust Heat. Part 2: Detailed Design and Analysis”. *Proceedings of the Institution of Mechanical Engineers, Part D: Journal of Automobile Engineering* 220(7), pp. 973–989. DOI: 10.1243/09544070jauto222. URL: https://dx.doi.org/10.1243/09544070jauto222.

Liu, S, Y Zhang, and P Liu (2008). “New analytical model for heat transfer efficiency of metallic honeycomb structures”. *International Journal of Heat and Mass Transfer* 51, pp. 6254–6258.

Loh, W. S. et al. (2009). “Adsorption cooling cycles for alternative adsorbent/adsorbate pairs working at partial vacuum and pressurized conditions”. *Applied Thermal Engineering* 29(4), pp. 793–798. DOI: 10.1016/j.applthermaleng.2008.04.014. URL: https://dx.doi.org/10.1016/j.applthermaleng.2008.04.014.

Liu S, Zhang Y, Liu P (2008) New analytical model for heat transfer efficiency of metallic honeycomb structures. International Journal of Heat and Mass Transfer 51:6254–6258

Saha, B. B. et al. (2003). “Waste heat driven dual-mode, multi-stage, multi-bed regenerative adsorption system”. *International Journal of Refrigeration* 26(7), pp. 749–757. DOI: 10.1016/s0140-7007(03)00074-4. URL: https://dx.doi.org/10.1016/s0140-7007(03)00074-4.

Saleh, Majdi M. et al. (2020). “Wire fin heat exchanger using aluminium fumarate for adsorption heat pumps”. *Applied Thermal Engineering* 164, pp. 114426–114426. DOI: 10.1016/j.applthermaleng.2019.114426. URL: https://dx.doi.org/10.1016/j.applthermaleng.2019.114426.

Singh H, Cai J (2018) A mechanistic model for multi-scale sorption dynamics in shale. DOI 10.1016/j.fuel.2018.07.104, URL https://dx.doi.org/10.1016/ j.fuel.2018.07.104

List of Figures

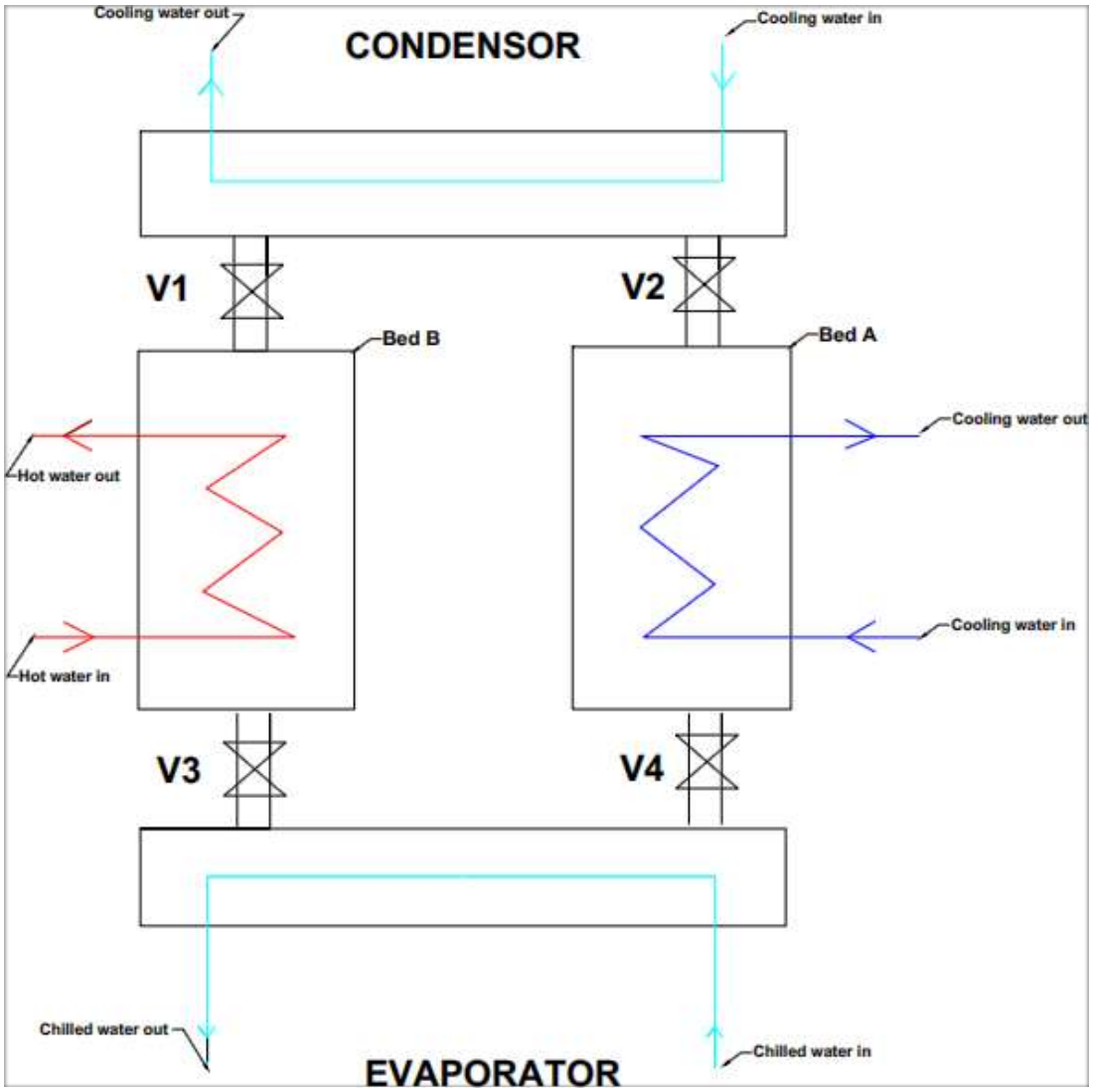

Fig. 1 Two-bed adsorption desalination cycle system.

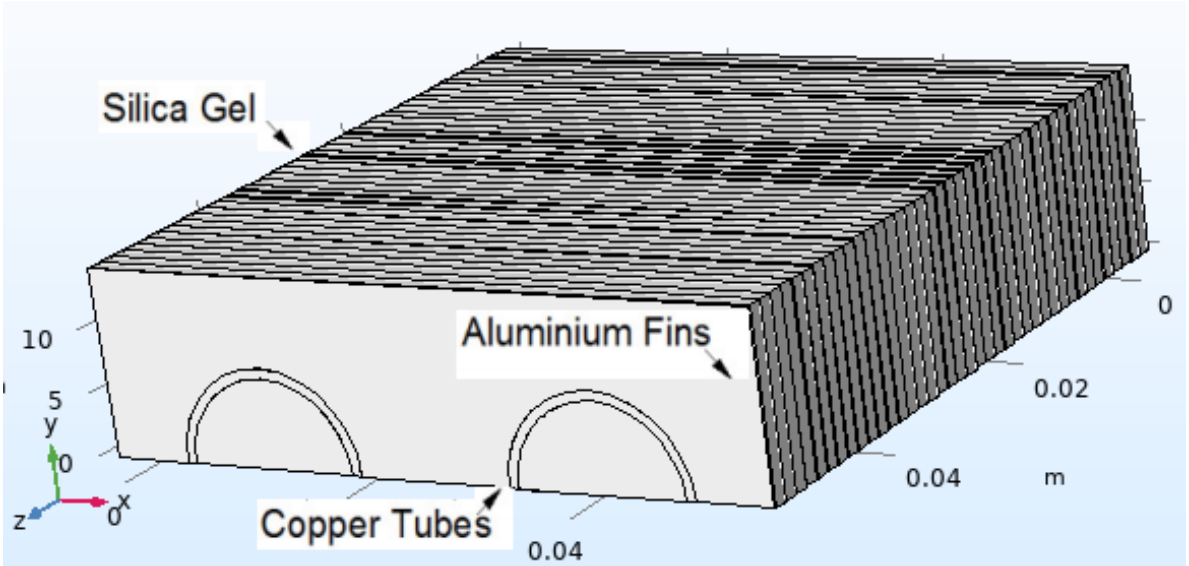

Fig. 2 Rectangular finned tube adsorption bed.

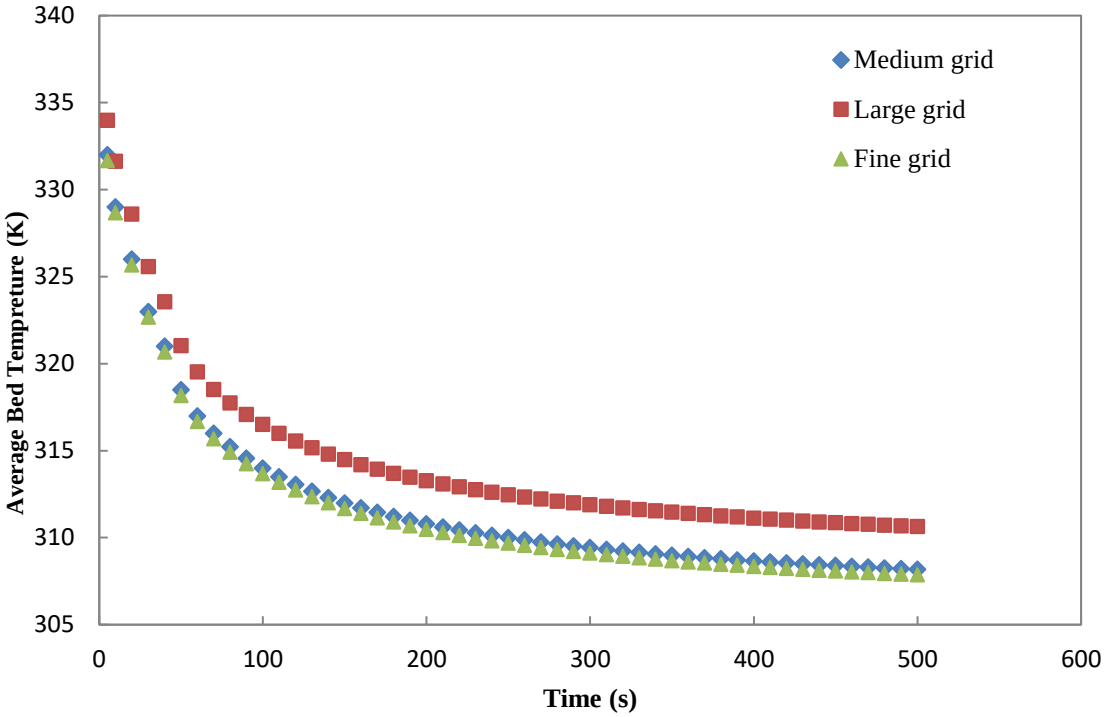

Fig. 3 Three mesh types analysis with different sizes (large-medium-fine).

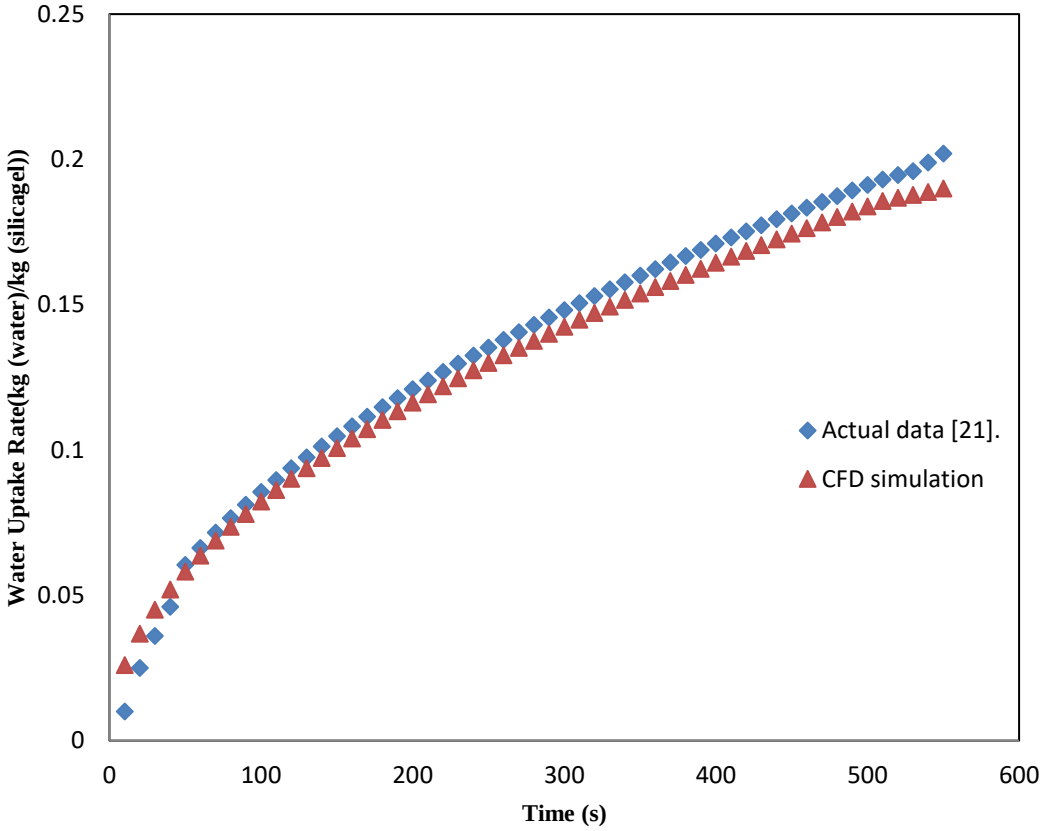

Fig. 4 Comparison of water vapour uptake between CFD predicted data and experimental data for SAPO-34/water working pair (Mass flow rate of 5 L/min) Shi et al. (2013) and Alsalman et al. (2017).

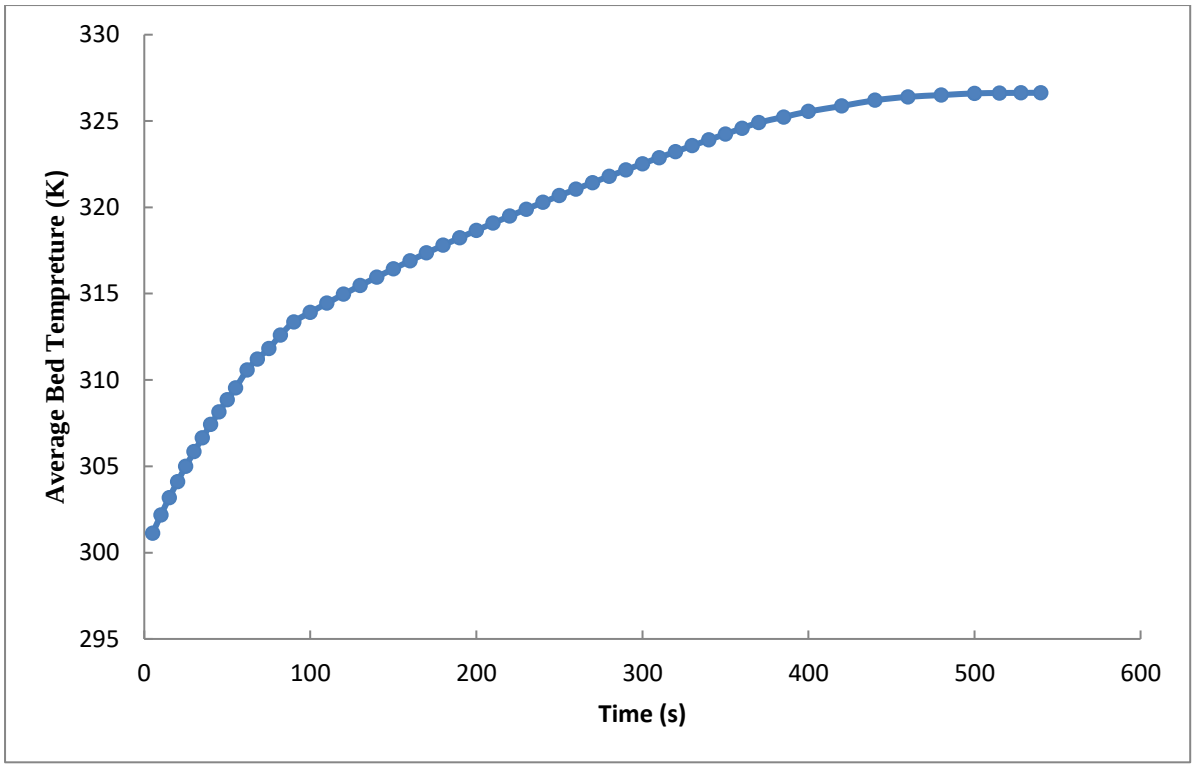

a)

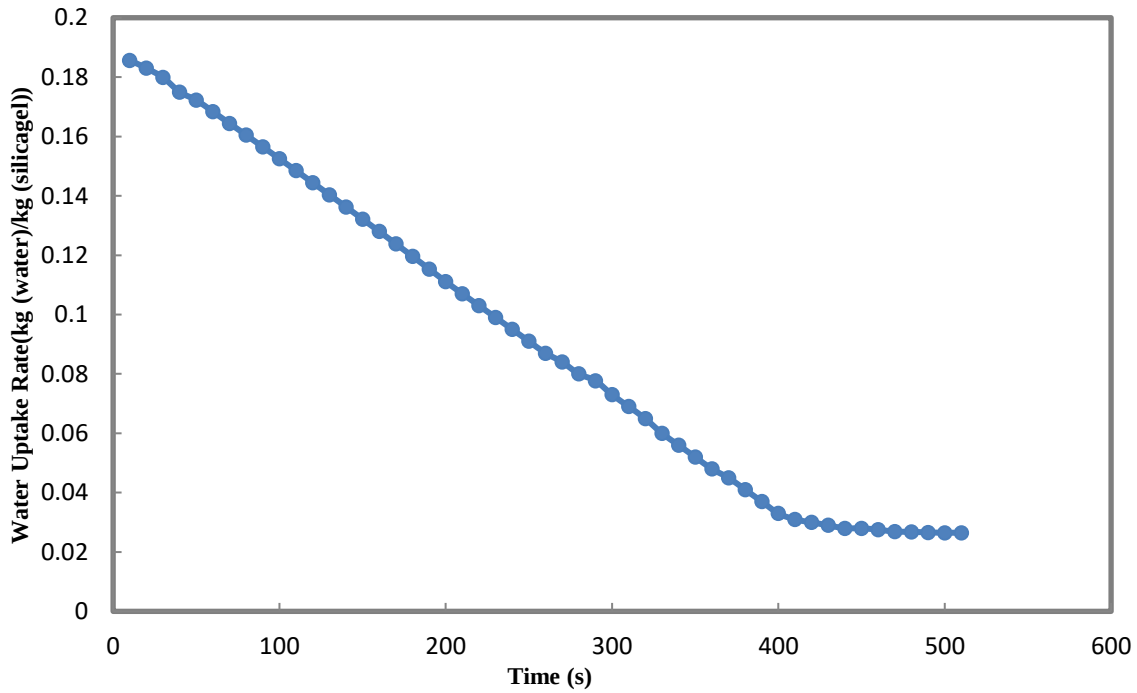

b)

Fig. 5 a. b. Simulation resultsfor adsorption process versus time: a) average bed temperature; b) water uptake rate

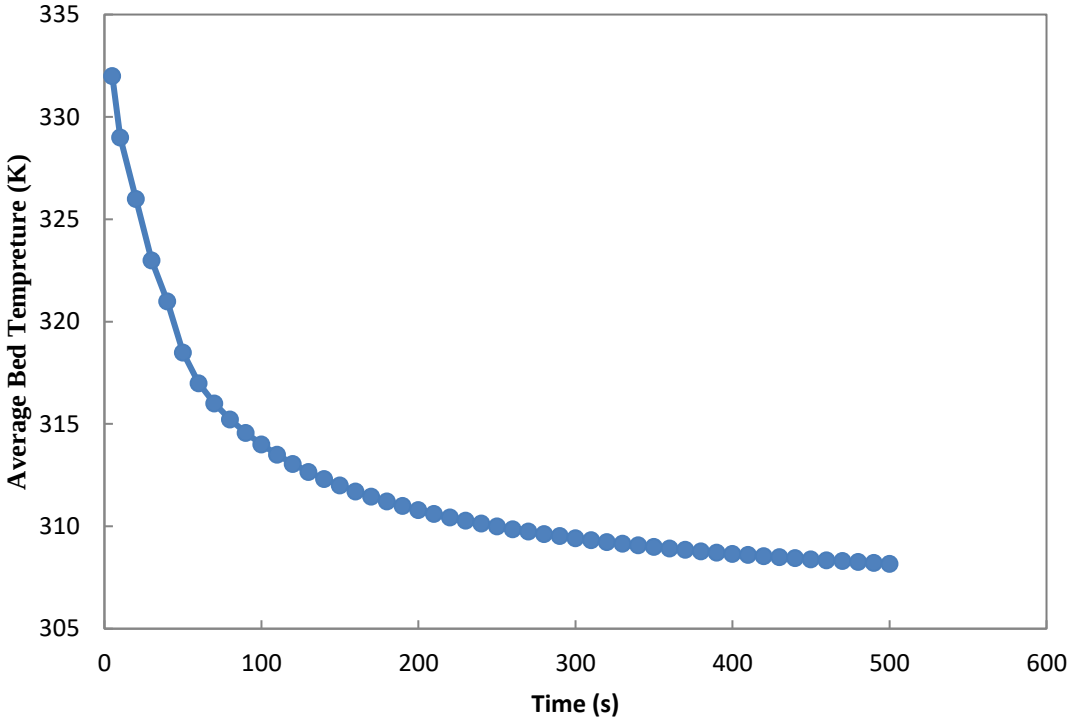

a)

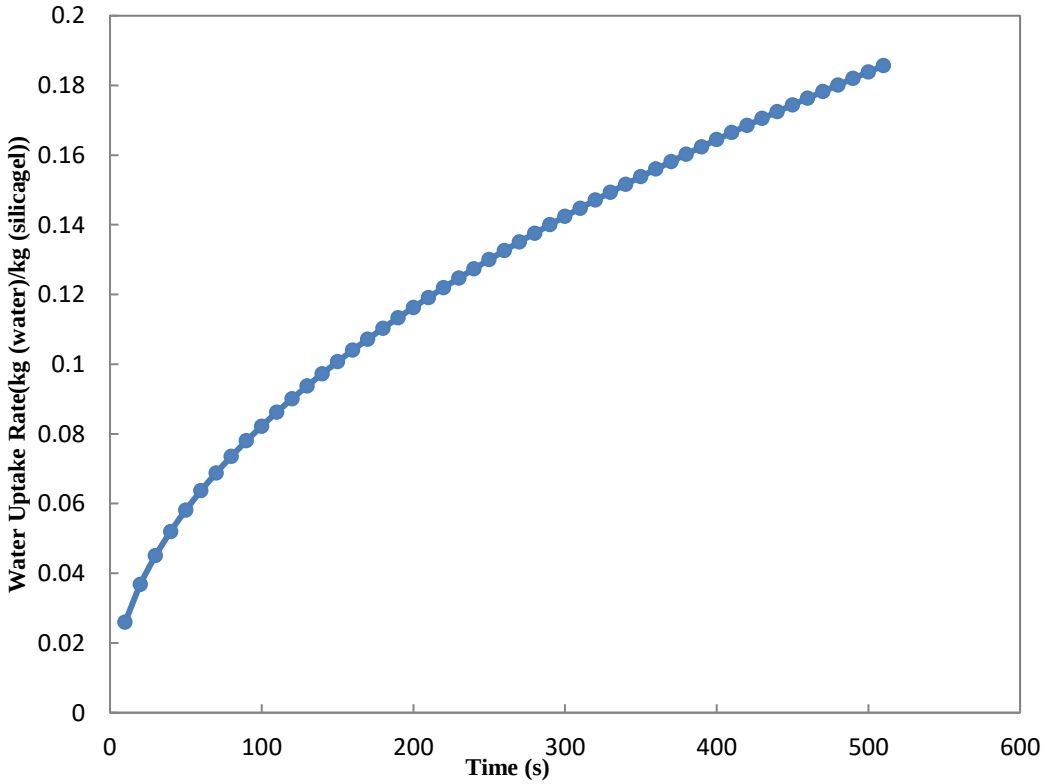

b)

Fig. 6 a. b. Simulation results for desorption process: a) average bed temperature; b) water uptake rate

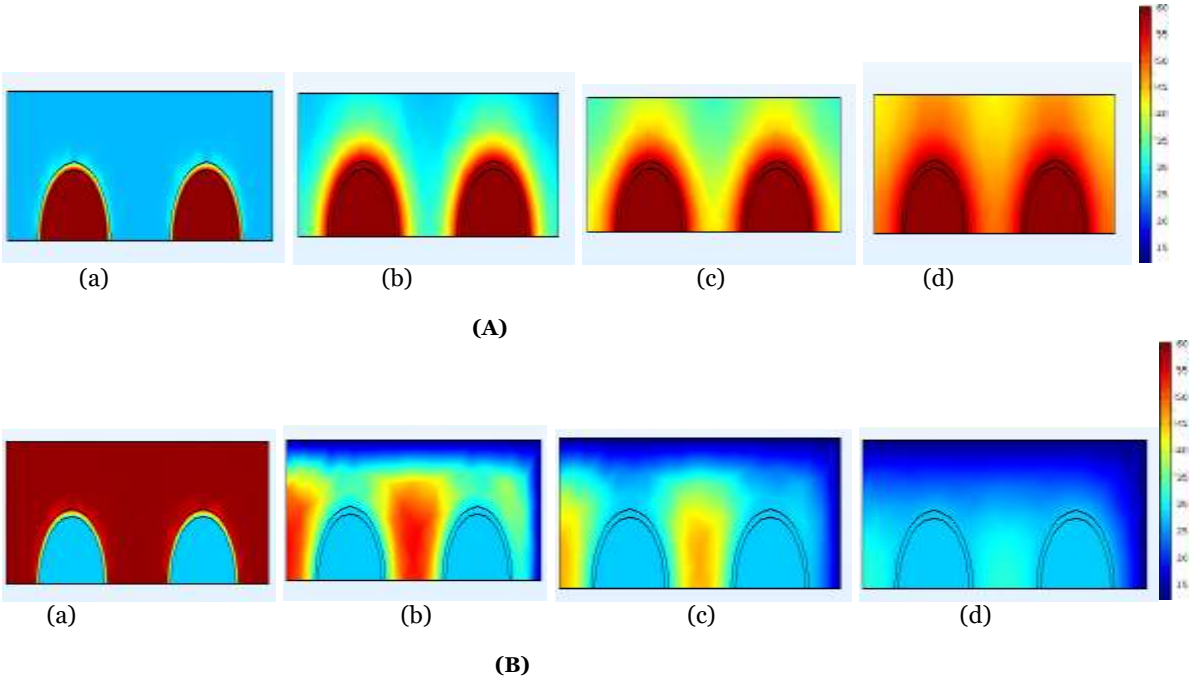

Fig. 7 A. B. Temperature distribution of the last fin at (a) 1s ; (b) 50s ; (c) 100s ; (d) 200s for desorbtion (A) and for adsorption (B)

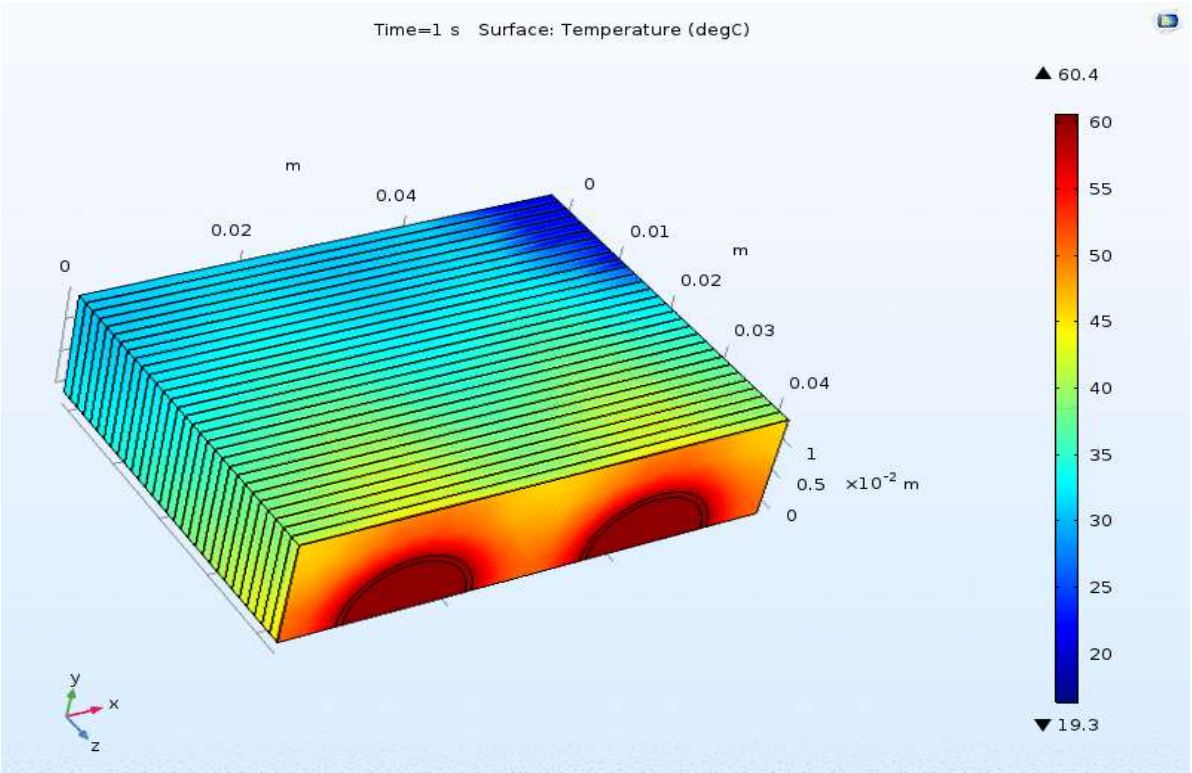

Fig. 8 Temperature distribution of adsorption bed in desorption process

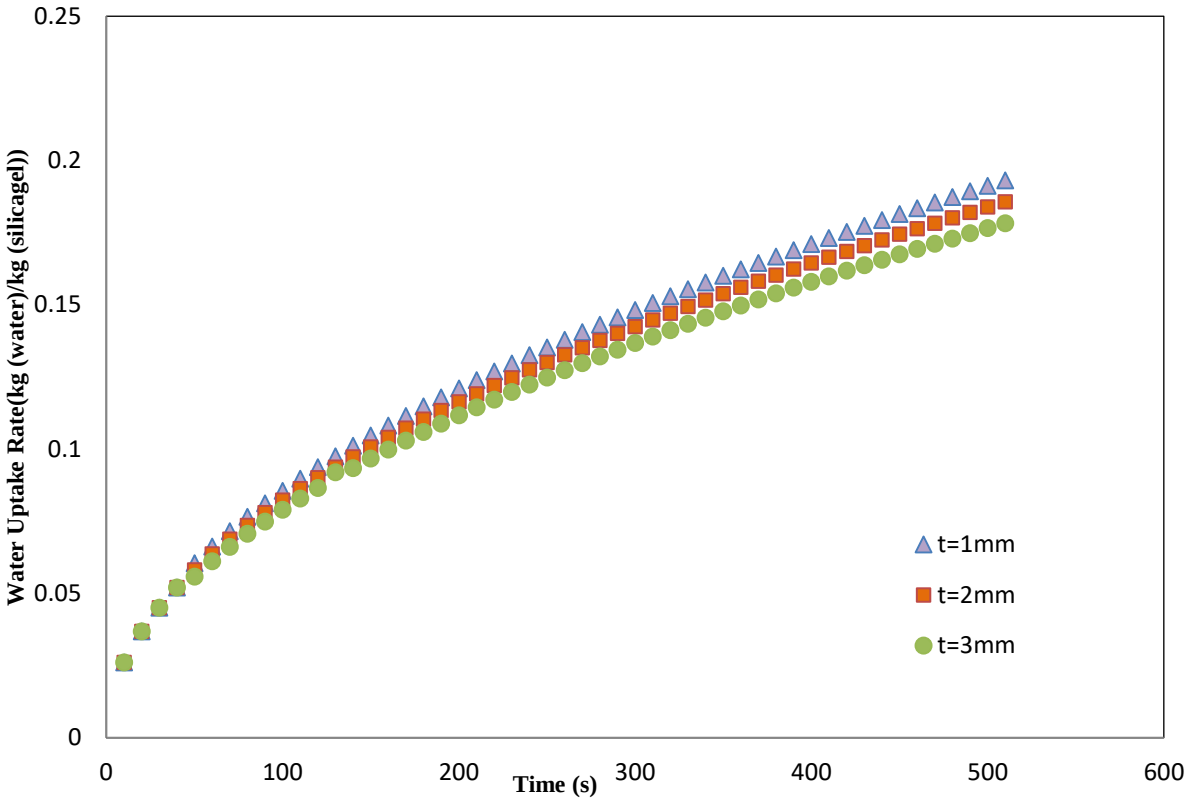

Fig. 9 Simulation results for water uptake rate with different fin thickness

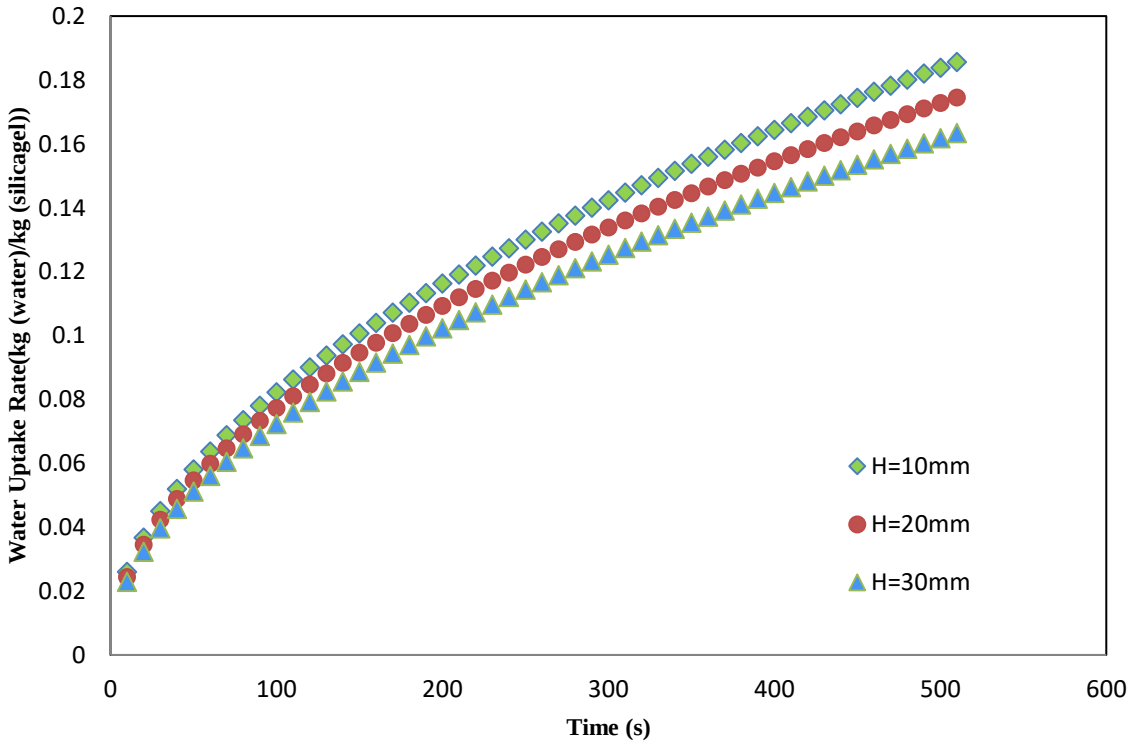

Fig. 10 Simulation results for water uptake rate with different fin heights.

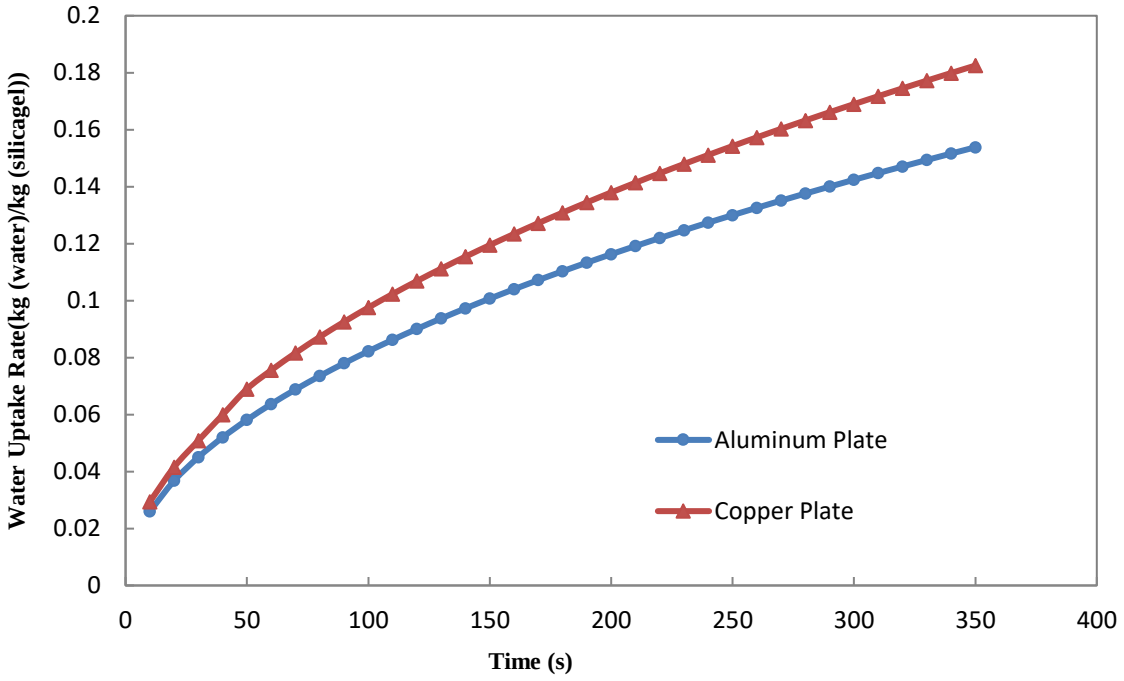

a)

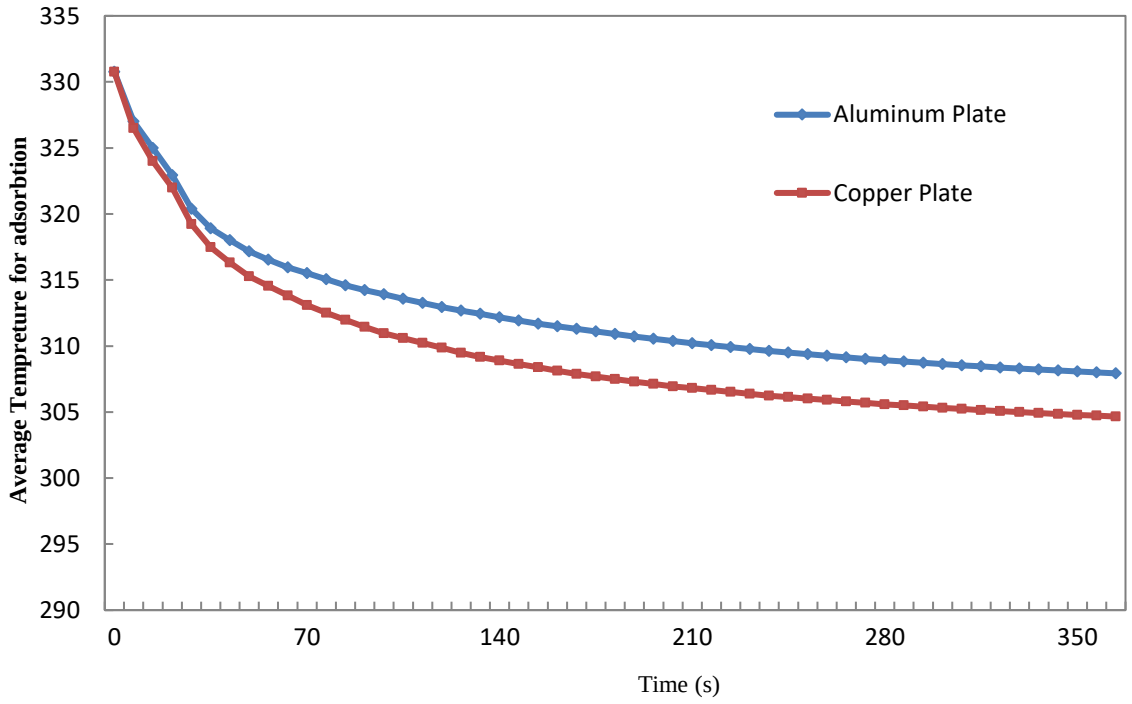

b)

Fig. 11 a. b. Simulation results for adsorption process with different plates types; a) Water uptake rate, b) average bed temperature

List of Tables

Table 1 Bed Design Parameters

Symbol	value	Description
L_f	100mm	Bed Length
W_f	115mm	Fin Width
H_f	30mm	Fin Height
P_f	1.5mm	Fin Pitch
t_f	0.105mm	Fin Thickness
D_0	15.8mm	Tube Outer Diameter
t_t	0.8mm	Tube Thickness

Table 2 Parameters for mass transfer rate equation.

Parameters	value	Unit
D_{so}	2.54×10^{-4}	m^2/s
E_a	4.2×10^{-4}	J/mol
R_p	0.15×10^{-3}	m
R	8.314	$J/(mol.k)$

Table 3 Constantsfor equilibrium uptake equation Saleh (2020).

Parameters	**value**	**Unit**
A_0	-6.531	$kg_{water}/kg_{silicagel}$
A_1	7.24×10^{-2}	$kg_{water}/(kg_{silicagel}.k)$
A_2	-2.39×10^{-4}	$kg_{water}/(kg_{silicagel}.k^2)$
A_3	-2.54×10^{-7}	$kg_{water}/(kg_{silicagel}.k^3)$
B_0	-15.58	1
B_1	0.159	K^{-1}
B_2	-5.06×10^{-4}	K^{-2}
B_3	-5.3×10^{-7}	K^{-3}